

## DISTANT CLUSTERS OF GALAXIES DETECTED BY X-RAYS

A. CAVALIERE

Astrofisica, Dipartimento di Fisica II Università di Roma, via della Ricerca Scientifica 1, I-00133 Roma, Italy

S. COLAFRANCESCO

Osservatorio Astronomico di Roma, Via dell'Osservatorio, I-00040 Monteporzio, Roma, Italy

AND

N. MENCI

Astrofisica, Dipartimento di Fisica II Università di Roma, via della Ricerca Scientifica 1, I-00133 Roma, Italy

Received 1991 May 24; accepted 1992 October 23

## ABSTRACT

The dynamical masses of groups and clusters of galaxies decrease on average with increasing redshift, after the hierarchical cosmogonies dominated by direct collapses of dark matter overdensities. We show that the masses of intracluster plasma emitting in the X-ray band are to decrease more rapidly. We also show that consideration of the intrinsic spread in the dynamical formation times leads us to predict more numerous faint sources at given dynamical mass. The model we compute yields steeper luminosity functions in the X-ray band with a specific change in lookback time: the bright end shifts back. Such negative evolution is fast even at modest redshifts  $z \lesssim 0.5$  if the external gas infalling into groups of clusters was preheated and has cooled down after  $z \approx 1.5$ – $2$ . If so, the evolution is considerably faster in the X-ray than in the optical band and compares interestingly with the data from the existing surveys.

*Subject headings:* galaxies: clustering — X-rays: galaxies

## 1. INTRODUCTION

Interest in the evolution of galaxy clusters has been recently rekindled by some apparent mismatch between the optical and the X-ray observations.

In the optical band, the present data suggest that the number density of clusters with large velocity dispersions declines only weakly, if at all, out to redshifts  $z \sim 0.8$  (Gunn 1990; Ellis 1991). But the present surveys still contend with small-number statistics, with velocities often limited to core galaxies, and with possible contaminations by projected groups (see discussions in the previous references and by Frenk et al. 1990 and Olivier et al. 1990).

The X-ray surveys, on the other hand, could single out physical potential wells of sizes  $R \sim \text{Mpc}$  associated with dynamical masses  $M \sim 10^{13}$ – $10^{15} M_{\odot}$ , out to  $z \approx 0.5$ – $1$ . They take advantage of the powerful, extended bremsstrahlung emission (Cavaliere, Gursky, & Tucker 1971; Gursky et al. 1972; Solinger & Tucker 1972) common to most local clusters and to many groups, with bolometric emission that scales like

$$L \propto n^2 \hat{R}^3 T^{1/2} \quad (1.1)$$

in terms of density  $n$ , size  $\hat{R}$ , and temperature  $T$  of the intracluster plasma (ICP). The outputs reach up to several  $10^{45}$  ergs  $s^{-1}$  from rich clusters, involving large masses  $\hat{M} \sim 10^{-1} M$  of ICP with central densities  $n \sim 10^{-3} \text{ cm}^{-3}$  heated up to virial energies  $kT \sim GMm_H/10 R \sim \text{several keV}$ . Moreover, the X-ray luminosities are less liable to contaminations from projection effects, being nonlinear with  $M$  or  $n$ .

But the first such survey to reach a substantial depth (Gioia et al. 1990; Henry et al. 1992; see also the independent data of Edge et al. 1990) indicated a dearth of luminous cluster sources already at  $z \gtrsim 0.2$ . These observations provided  $z$ -resolved luminosity functions (LFs) which are steep over a range of more than a decade; a shape consistent, in fact, with that of the

local LF of Piccinotti et al. (1982) and Kowalski et al. (1984) at higher photon energies. The picture resulting from these data is one where steep LFs shift rapidly to lower luminosities with increasing  $z$  (negative “luminosity evolution”).

While awaiting conclusive results from the *ROSAT* surveys (Trümper et al. 1991; Böhringer et al. 1991), we discuss what conditions may govern the actual X-ray evolution. The theoretical expectations based on scale-invariant hierarchical clustering (Kaiser 1986) predicted a strong increase in source number (“density evolution”) with increasing  $z$ , with a slower luminosity decrease. Cavaliere & Colafrancesco (1988, 1990) pointed out that  $\hat{M}/M$ , the relative content in ICP of clusters and groups, is likely to increase both in cosmic time and with  $M$ , hence the X-ray luminosities are bound to undergo a faster negative evolution in lookback time. In this paper we derive the  $z$ -dependent LFs combining the two *astrophysical* components: clustering dynamics and ICP physics.

The clustering dynamics considered in the body of paper is described in § 2. We treat the physics of the ICP in § 3: § 3.1 deals with the gas mass available per unit dynamical mass; § 3.2 deals with the role of the external and internal temperatures in setting the central ICP density, so governing the luminosities. In § 4 we consider the effects of the intrinsic density dispersion on the shape of the LFs. We then compute the complete LFs embodying both the effects discussed in §§ 3 and 4. An alternative dynamical framework is discussed in § 5. In the final section we summarize our findings and their implications.

## 2. DYNAMICAL AND ICP QUANTITIES

The X-ray luminosity by optically thin, thermal bremsstrahlung emission is written in equation (1.1) in terms of ICP parameters, but these may be related to dynamical quantities. Density  $n$  and mass  $\hat{M}$ , or size  $\hat{R} \propto (n/\hat{M})^{1/3}$ , are related to their dynamical counterparts, namely, average internal density  $\rho$

and virial mass  $M$ , or dynamical size  $R \propto (M/\rho)^{1/3}$ . Moreover, in virial equilibrium the ICP temperature satisfies  $T \propto M/R$  (and the electrons reach equipartition with the ions). Likewise, the LF may be related to the mass distribution (MD) associated with the dynamical structures. We shall see that these relationships are not straightforward and require discussion.

### 2.1. Dynamical Framework

We consider first the canonical clustering scenario based on direct hierarchical collapses (DHCs). This envisages a field of small initial overdensities  $\delta \equiv \delta\rho/\rho$ , gravitationally unstable to form condensations of high contrasts  $\delta \gtrsim 2 \times 10^2$ . The linear  $\delta$  are taken to constitute a random-phase Gaussian field: power spectrum  $\langle |\delta_k|^2 \rangle \propto k^\nu$ , with  $-3 < \nu < -1$  at cluster and group scales; distribution on a given mass scale  $p(\delta|M) \propto \exp(-\delta^2/2\sigma^2)/\sigma$ , with  $\sigma \propto M^{-a}$  and  $a \equiv (\nu+3)/6$  (see Peebles 1980).

The gravitational instability is weak even in a high-density FRW universe, with the relatively slow growth  $\delta(z) \propto (1+z)^{-1}$  as long as  $\Omega \approx 1$  holds. On crossing a threshold of nonlinearity  $\delta_c \sim 1$ , the perturbations collapse and settle to a virial equilibrium in a few dynamical times corresponding in the extrapolated linear development to an effective threshold  $\delta_c \approx 1.7$ . The characteristic mass virializing at  $z$  for a typical overdensity (spherical, homogeneous, with amplitude  $\delta \sim \sigma$ ) is progressively larger with decreasing  $z$  and follows the strong law  $M_c(z) \propto (1+z)^{-1/a}$  in a critical universe. The present value is taken  $M_c(0) \approx 10^{15} h_{50}^{-1} M_\odot$ , corresponding to a richness 1 cluster as defined by Abell (1958). The internal densities scale like the background,  $\rho \sim 2 \cdot 10^2 \rho_a \propto (1+z)^3$ ; the sizes as  $R_c \propto (M/\rho)^{1/3} \propto M_c^{(5+\nu)/6}$ ; and the specific virialized energies like  $V^2 \propto M/R \propto M_c^{(1-\nu)/6}$ . We consider FRW universes with  $H_0 = 50 \text{ km s}^{-1} \text{ Mpc}$ , and with  $\Omega_0 = 1$  up to § 6.

Such a scenario, envisaging scale-free collapses from a field with a scale-free power spectrum, naturally leads to MDs with scale-invariant (and self-similar) form. In fact, such form reads (Cavaliere, Colafrancesco, & Scaramella 1991)

$$N(M, z) \propto M_c^{-2}(z) m^{-\Gamma} e^{-\beta m^\Theta}, \quad (2.1)$$

where  $m \equiv M/M_c$ . The parameters take on the values  $\Theta = 2a$  and  $\Gamma = 2 - a$  in the specific model derived first by Press & Schechter (1974), where  $\beta$  takes on the value  $\delta_c^2/2$ . When the spectrum is normalized to, for example,  $\sigma(16 h_{50}^{-1} \text{ Mpc}) = 1/b$  (Kaiser 1984),  $\beta$  takes on the value  $b^2 \delta_c^2/2$ .

### 2.2. The Simple Link with the ICP

The important point is that the simplest relationships of ICP with dynamical quantities fail to comply with the existing evidence. In fact, equal scalings for ICP as for dynamical quantities, namely,  $n \propto \rho$  and  $\hat{R} \propto R \propto (M/\rho)^{1/3}$ , lead to the result

$$L \propto M^{4/3} \rho^{7/6}. \quad (2.2)$$

This fully scale-invariant model (Kaiser 1986) implies that the decrease toward higher  $z$  of the characteristic luminosity  $L_c(z) \propto M_c^{4/3}(z) \rho^{7/6}(z) \propto (1+z)^{(5+\nu)/(v+3)}$  is slower than the decrease of  $M_c(z)$ , due to the increase of  $\rho(z)$ .

Similarly, the X-ray LFs may be derived from the MD in equation (2.1) simply with the transformation  $L \propto M^{4/3}$  from equation (2.2), or more generally from  $L \propto M^c$ . The result is

$$N(L, z) \propto M_c^{-1}(z) L_c^{-1}(z) \ell^{-\gamma} e^{-\beta \ell^\theta}, \quad (2.3)$$

where  $\ell = L/L_c(z)$ ; for the Press & Schechter (1974) model,  $\theta = 2a/c$  and  $\gamma = 1 + (1-a)/c$  hold.

### 2.3. Problems

The above LF has three generic features: the logarithmic slope at the faint end is rather flat with  $\gamma \lesssim 1.6$ , while the upper cutoff steepens with increasing  $b$  and softens for decreasing  $\nu$ ; with  $z$  increasing, the shape is self-similarly conserved, but the luminosities recede following the decrease of  $L_c(z)$  (negative luminosity evolution); the integrated source number increases more strongly like  $M_c^{-1}(z)$  (density evolution). The amplitude of the LF scales following  $N(z) \propto L_c^{-1}(z)/M_c(z)$ ; thus the strong density evolution  $M_c^{-1}(z)$  dominates the body of the distribution for  $\nu > -2.4$  to yield nearly superposed LFs out to  $z \approx 0.3$ , as shown by the dotted curve in Figure 3.

Instead, the present  $z$ -resolved data referred to in § 1 suggest a strongly negative luminosity evolution, fast enough as to cause an appreciable dearth of bright sources over the range  $z \approx 0-0.3$ .

So the present evidence calls for nontrivial solutions concerning both the dependence  $L_c(z)$  and the shape of the LFs. We tackle these points in turn.

## 3. THE HISTORY OF THE ICP

If the clustering by DHC is to be retained, then one has to give up one, or both, of the simple scalings  $n/\rho = \text{const}$  and  $\hat{R} \propto R$ . The latter is consistent with structures fully dominated by dark matter which imposes on the virialized ICP its own scaling and is retained (see § 5). But the history of the ICP can give rise to a variable ratio  $n/\rho \equiv g(M, z)$ , leading to the full dependence of the luminosity given by

$$L \propto g^2(M, z) M^{4/3} \rho^{7/6}. \quad (3.1)$$

We take up the proposal by Cavaliere & Colafrancesco (1988), that most ICP constitutes a younger cluster component than the dynamical mass. Recent evidence bearing on the origin of the ICP include the following: The ratio gas/stars rises from  $\hat{M}/M_* \lesssim 10^{-2}$  in X-ray galaxies (see Trinchieri & Fabbiano 1985; Fabbiano 1989) to  $\sim 1$  in groups, up to values  $\sim 5$  in rich clusters (Blumenthal et al. 1984; David et al. 1990); we fit the data with  $\hat{M}/M \propto M^{0.2}$  in the range  $M \sim 10^{14}-10^{15} M_\odot$ . The definitely subsolar Fe/H  $\sim 0.3-0.4$  in rich clusters (see Edge & Stewart 1991a, b) requires abundant dilution with unprocessed baryons of the high yields (Fe/H) $_*$  from elliptical galaxies which are predicted by many stellar evolutionary models (see, e.g., Ciotti et al. 1991). Finally, in the optical band the ratio  $M/L_0$  is believed to increase with  $M$ , on gross average like  $M^{1/4}$  or  $M^{1/3}$  (see, e.g., Hoffman, Shaham, & Shaviv 1982). These facts may be connected as follows.

The initial star populations in early galaxies used up much of the initial baryons. The associated nuclear energy gave rise to strong winds from SN II and later from SN I, with velocity  $v_w$ . These swept clear of residual gas the shallow potential wells of galaxies and of small groups, up to a mass scale  $M_1$  such that the associated velocity dispersion satisfies  $V^2(M_1) \sim v_w^2$  (see, e.g., David et al. 1990). The winds built up a considerable pressure of nongravitational origin even in somewhat deeper wells, thus holding at bay the diffuse baryons.

Later on, when progressively deeper and larger wells collapse, mass from relatively underdense regions is accreted or engulfed. The gravitational range for accretion extends out to progressively larger distances  $R[M/M_c(z)]^{w/3}$  with  $\frac{1}{2} \lesssim w < 1$ , marking the radius where coherence is destroyed by the rms noise on smaller scales. Thus large, stratified halos are accreted with masses  $M_h = M[M/M_c(z)]^w$  (Cavaliere et al. 1991).

Biased light distribution (see Cole & Kaiser 1989) and initially uniform baryon density imply the outer material, including failing galaxies, to be darker and to contain a larger proportion of free baryons versus those clumped into stars. On infall into the large wells, the free baryons are heated up by release of gravitational energy.

Incidentally, suppressing or preventing star formation by nuclear and then by gravitational heating (except in localized cooling flows; see Sarazin 1988; Fabian 1991) has two related consequences: light biasing is sustained or amplified by dynamic biasing, and a large fraction of baryons is left over to feed the ICP.

The net result relevant for the X-ray emission is that *nuclear* energy set a mass scale of order  $M_1 \lesssim 10^{13} M_\odot$  where the ratio  $\hat{M}/M$  was minimal. We argue that the recovery toward higher relative contents of ICP was *slow*.

### 3.1. Baryons Available

The increasing content in diffuse baryons available for higher levels of the collapse hierarchy, and the associated increase of  $L/M$ , is *complementary* to the decrease of  $L_0/M$ . This may be computed combining  $M/L_0 \propto M^{1/4}$  with  $\hat{M} + M_* = \Omega_b M$  independent of scale. Thus one recovers the empirical  $\hat{M}/M \propto M^{0.2}$  in the range  $M \sim 10^{14}-10^{15} M_\odot$ .

The role of the halos, little visible in X-rays because of their low surface brightness, is that of temporary reservoirs of diffuse baryons, to be partly incorporated into the ICP at next reshufflings when halos and central regions get mixed in the collapse of new central regions. The decrease of the relative stellar content in such central regions, or the complementary increase in *available* gaseous content, may be followed with simple models of stepwise dilution.

Consider, for simplicity, that a central region of the  $i$ th generation is comprised of material from previous central regions and from previous halos, in a ratio proportional to the respective typical masses  $M_i = \epsilon M_{i-1} [1 + (M_{i-1}/M_c)^w]$ . The value  $(M_{i-1}/M_c)^w$  is taken to be nearly constant at values  $\approx 1.5-1.7$ , in accord with the broad maximum in the probability distribution of density peaks (see Bardeen et al. 1986).

Starting with an initial central region consisting only of stellar material, after  $i$  steps in this discrete hierarchy the stellar content is

$$\frac{M_*}{M} = \frac{1}{\epsilon^{i/w/a}}. \quad (3.2)$$

For the complementary quantity  $\hat{M}/M \propto g$  we then obtain

$$g(M) \propto \Omega_b \left(1 - \frac{M_*}{M}\right) \propto M^{0.3} - M^{0.2}, \quad (3.3)$$

flattening over the mass range  $10^{13}-10^{15} M_\odot$ . The exponents range from somewhat flatter when also field baryons are involved, to somewhat steeper for a mass step smaller than the value  $\sim 2$  adopted above.

The above arguments, which picture the groups and clusters as systems *open* to external gas mixing, reproduce the relative increase of  $\hat{M}$  by a factor  $\hat{M}/M \sim 5$  in the mass range  $2 \times 10^{13}-10^{15} M_\odot$  observed by David et al. (1990).

### 3.2. The ICP Compression

A further dependence of  $g$  comes from the varying fraction of the available gas which can be compressed into the potential

wells. Many numerical simulations (from Perrenod 1978, to Evrard 1990) have shown that, when the infalling gas temperature (or entropy) is smaller than the virial temperature (or final entropy) associated with the potential well, a shock front forms, and moves outward leaving inside a nearly hydrostatic and isothermal distribution of density, which joins to the inner boundary condition at the shock.

The density  $n_2$  at the inner boundary, as a function of the external  $n_1$  and of the temperature ratio  $T_1/T_2$ , may be computed as follows. The Hugoniot adiabat provides the compression factor

$$n_2/n_1 = 2(1 - T_1/T_2) + [4(1 - T_1/T_2)^2 + T_1/T_2]^{1/2} \quad (3.4)$$

for pointlike particles (see Landau & Lifshitz 1959). As is well known, this is very close to the Poisson adiabatic compression for weak shocks when  $T_2 \gtrsim T_1$ , but saturates to  $n_2/n_1 \rightarrow 4$  for strong shocks when  $T_2 \gg T_1$ .

For an analytical evaluation, consider that  $T_2$  increases on average while  $T_1$  will decrease for  $z \lesssim$  a few, as the thermal inputs die out. So the ratio  $T_1/T_2$  is a direct function of  $z$ , while  $g(z) \propto n_2/n_1$  will be an *inverse* function of  $z$  approaching unity for  $M_c(z) \sim M_1$  (see Fig. 1). Actually, the approximate equality  $T_1 \sim T_2$  may be maintained down to a redshift  $z_1 = 1.5-2$  because part of the gas involved in condensations was previously held in preceding halos, while powerful energy inputs are still contributed by SN type I activity decaying like  $t^{-1.3}$  (see discussion by Ciotti et al. 1991).

Eventually, the external temperature drops nearly adiabatically following  $T_1 \propto (1+z)^2$  for baryons subjected to pure Hubble expansion; the other reference case  $T_1 \approx \text{const}$  yields similar results, as shown in Figure 1. Meanwhile the virial temperatures still go up following on average  $T_2 \propto (1+z)^{(v-1)/(v+3)}$ .

We note that the central density is related to  $n_2$  by the shape factor given by the model of Cavaliere & Fusco-Femiano (1976). This involves only one additional parameter  $V^2/T_2$ , taken to be approximately constant.

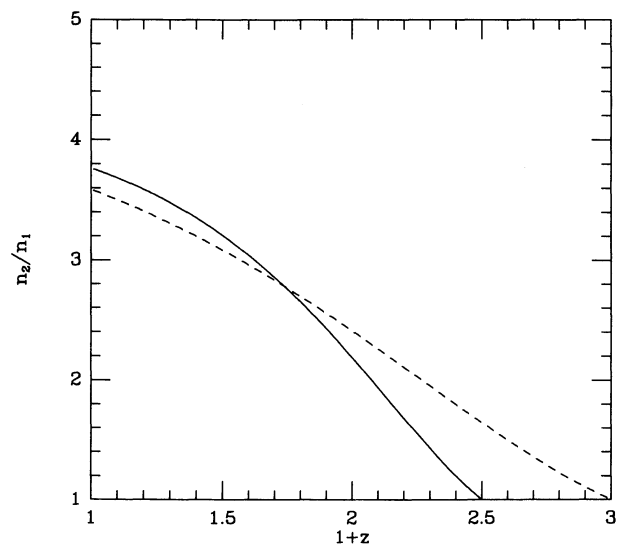


FIG. 1.—The  $z$ -dependence of the compression ratio  $n_2/n_1$ , defined in the text. The continuous line refers to the case  $T_1 \propto (1+z)^2$ , with  $z_1 = 1.5$ . The dashed line illustrates the behavior for the reference case  $T_1 \sim \text{const}$ , with  $z_1 = 2$ . Note that the slopes for  $z \lesssim 0.5$  are close.



The above  $z$ -dependences inserted into equation (3.4) yield for  $n_2/n_1$  the results plotted in Figure 1. This shows that the  $z$ -behavior of  $n_2/n_1 \propto (1+z)^{-\xi}$ , with  $\xi \approx 0.5-1$  depending on  $z_1 \approx 2-1.5$ , constitutes an efficient approximation in the range  $z \sim 0.1-0.3$ . The complete scaling

$$g(M, z) \propto m^{0.2} M_c^{0.2} (1+z)^{-\xi} \quad (3.5)$$

may be used to evaluate  $L_c(z)$  after equation (3.1). The result is a strong negative evolution of  $L_c(z) \propto (1+z)^{(5+7\nu)/(2\nu+3) - 2.4/(\nu+3) - 2\xi}$ .

#### 4. THE LUMINOSITY FUNCTION

As to the shape of the LFs, we argue that the simple transformation  $L \propto M^c$  is incomplete. This is indicated by the following argument. The luminosities (2.2) depend strongly not only on  $M$ , but also on the density at formation  $\rho_f \propto (1+z_f)^3$ , and so they are bound to amplify any spread existing in the formation epochs  $z_f$ . An intrinsic spread arises because in the DHC clustering  $z_f$  is set by the initial  $\delta$  following

$$\rho(z_f) \propto \rho(z) \left( \frac{1+z_f}{1+z} \right)^3 \propto \rho(z) \delta^3, \quad (4.1)$$

and the  $\delta$  are distributed according to  $p(\delta | M)$ . Consistently, on the basis of equation (3.5) we consider that

$$g(M, z_f) = g(M, z) \delta^{3.5 - 2\xi - 0.2/a}. \quad (4.2)$$

As a result, the scaling for the luminosity is

$$L \propto g^2(M, z) M^{4/3} \rho(z)^{7/6} \delta^d, \quad (4.3)$$

with  $d = 7/2 - 2\xi - 0.4/a \approx 0.5$ .

The additional  $\delta$ -dependence will not change the behavior of  $L_c(z)$ , but will modify the shape of the LF at given  $z$ . We expect at the faint end an excess at given mass, due to additional sources with larger  $\delta$ . The knowledge of  $p(\delta | M)$  may be used in two ways. From equation (4.3) and from  $p(\delta | M)$  Cavaliere, Burg & Giacconi (1991) derived  $p(L | M)$ , the distribution of luminosities at given  $M$ , and its variant at given Abell mass. These distributions may be convolved a posteriori with the corresponding mass distribution (provided this is theoretically or empirically known) to derive a local LF.

Alternatively, we may consider the distributions in  $M$  and in  $\delta$  on equal footing, and derive specific forms of the LF directly from the initial density field. For example, we may parallel the deviation by Press & Schechter (1974), with consideration of the explicit  $\delta$ -dependence given by equation (4.3). Choosing  $L$  and  $\delta$  as independent variables, and considering the Gaussian form for  $p(\delta | \sigma)$ , we derive in the Appendix the number density of objects with a given luminosity  $L$  and with  $\delta > \delta_c$ , to read

$$N(L, z) = A \frac{\rho_a(z)}{M_c(z)L_c(z)} \left[ \ell^{-1 - (1-a)/c} e^{-b^2 \delta_c^2 \ell^{2a/c/2}} + C \ell^{-1 - 1/(c-ad)} \Gamma \left( q, \frac{b^2 \delta_c^2}{2} \ell^{2a/c} \right) \right] \quad (4.4)$$

where again  $\ell = L/L_c$ , the index  $q = [1 + d(1-a)/c] / 2(1-ad/c)$ , and the coefficients  $A \sim 1$  and  $C \sim 1$  are given in the Appendix.

The second term vanishes when no  $\delta$ -dependence for  $L$  is assumed (i.e., when  $d = 0$ ), and then one recovers the canonical expression in equation (2.3). Its power-law component has a

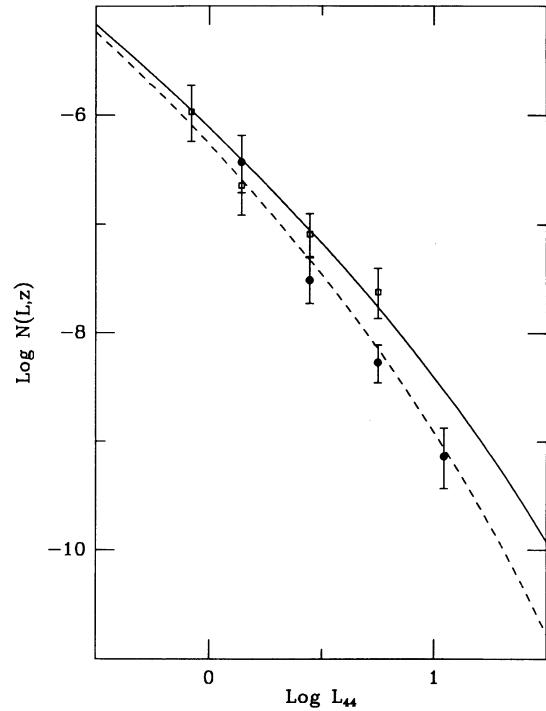


FIG. 2.—The X-ray LFs for local and for distant clusters and groups. These are computed from eq. (4.5) with  $g(M, z) \propto m^{0.2} M_c^{0.2} (z)n_2/n_1$ , and are plotted versus the luminosity reduced to the band 0.3–3.5 keV after Henry et al. (1992). Parameters:  $\Omega_0 = 1$ ,  $H_0 = 50 \text{ km s}^{-1} \text{ Mpc}$ ,  $\nu = -1.2$ ,  $b = 1.5$ . Normalization to the density of rich clusters derived by Scramella et al. (1990). The solid line corresponds to  $z = 0.17$ , and the dashed one to  $z = 0.35$ . A comparison is made with the *Einstein* data by Henry et al. (1992): the open squares refer to a bin centered at  $z \approx 0.17$ , and the filled squares to a bin centered at  $z \approx 0.35$ .

steeper slope  $1 + (c - ad)^{-1}$ , and the incomplete  $\Gamma$ -function by itself has a soft cutoff at the bright end but this is tilted down by the former.

Considering instead the distribution  $p(\delta | M)$  corresponding to the high-peak collapse (see Appendix), the result is similar with a slightly flatter slope at the faint end.

Inserting  $L_c(M, z)$  with its full dependencies derived in § 3 into equation (4.4) we compute numerically the  $z$ -dependent LFs, which are plotted in Figures 2 and 3. To compare with the data by Henry et al. (1992), the bolometric luminosity  $L$  has been converted to the 0.3–3.5 keV *Einstein* band following these authors; this implies an additional dependence  $M^{-0.12} (1+z)^{-0.18}$  in  $g(M, z)$  of equation (3.5). Figure 2 illustrates the LFs for  $\nu = -1.2$  and  $b = 1$ , with a strong ICP evolution ( $\xi = 1$ ); figure 3 is for  $\nu = -1.7$  and  $b = 1.2$ , with  $\xi = 0.5$ . For  $\nu > -1.2$  or  $\nu < -1.7$  the LFs result in being too steep or too flat, respectively.

#### 5. ALTERNATIVE SCENARIOS

The alternative way toward a strong negative evolution preserves the relationship  $\hat{M}/M \sim \text{const}$  and instead breaks the scaling for the sizes by assuming  $\hat{R} \sim \text{const}$ , to obtain

$$L \propto M^2 T^{1/2}. \quad (5.1)$$

However, within the DHC clustering scenario, such an assumption (Perrenod 1980) is not really consistent if the ICP

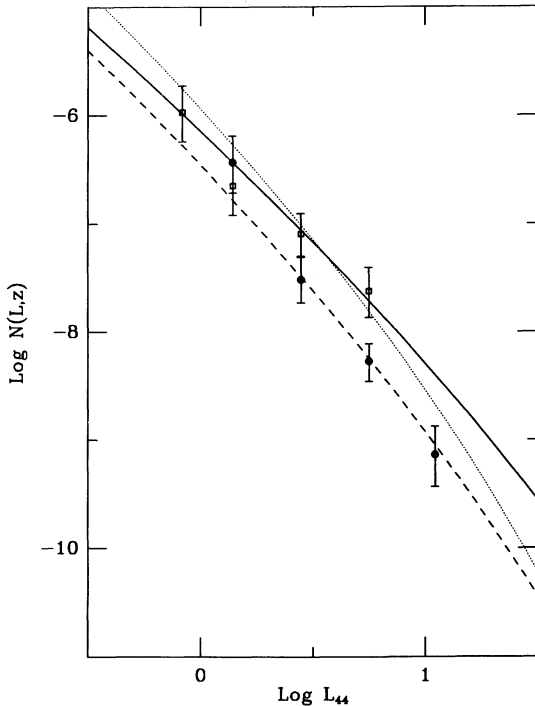


FIG. 3.—As in Fig. 2, for  $\nu = -1.7$  and  $b = 1.2$ . The dotted line corresponds to the LF of eq. (2.3) with  $g = \text{const.}$ , at  $z = 0.35$ .

in the central region follows an approximate hydrostatic equilibrium with  $V^2/T \sim \text{const}$  (Cavaliere & Fusco-Femiano 1976; Perrenod 1978; Evrard 1990), since then the emissivity then shares the dynamical scaling  $\bar{R} \propto R \propto M^{(\nu+5)/6}$ .

The assumption  $\bar{R} \sim \text{const}$  is more fitting in the context of the other way to build hierarchical structures, that is, by interactions and binary merging of smaller nonlinear units. This process is described in full by Cavaliere, Colafrancesco, & Menci (1991, 1992, hereafter collectively CCM).

The effective merging time  $\tau \propto 1/\bar{N}\langle\Sigma v\rangle \propto 1/\rho_a$ , where  $\rho_a$  is the average density of the ambient. Thus the evolutionary rate of the two-body aggregation processes is quite sensitive to the time dependence of the ambient density  $\rho_a(t)$ .

In a homogeneous field, the merging time increases strongly with  $t$ , because the ambient density decreases as  $\rho_a(t) \sim t^{-2}$  or faster. Then the evolution of the MD is self-similar but with a characteristic  $M_*(t)$  which grows slowly and soon comes to a standstill.

Even assuming a  $t$ -independent merging rate (see Edge et al. 1990) the evolution of  $M_*(t) \propto t$  is much slower than  $M_c(t) \propto t^2$ . This lazy pace hardly may be compensated in the X-ray by the strong acceleration of  $L_*(z)$  relative to  $M_*(z)$  implied by the strong dependence in equation (5.1). On the other hand,  $\bar{R} \sim \text{const}$  implies a strong decrease of  $T(z) \sim M_*(z)$ , and a dramatic decrease of all surface brightnesses.

However, our point is that a sustained merging rate will not hold in the field, where instead  $\rho_a \sim t^{-2}$  causes the characteristic mass to saturate soon. Aggregations are effective only in ambients where the density  $\rho_a(t)$  does not decrease too rapidly.

A favorable ambient for binary merging is constituted by gravitationally bound systems with characteristic mass  $M_c(z)$ ,

where interactions easily cause runaway formation of a single merger in a few dynamical times; this in fact is a description of the erasure of subclusters and groups within a forming cluster (CCM). The important point is that the ambient systems still form via DHCs; merging contributes erasure of internal structure and final amalgamation, with little room for strong shocks, and a possible breakdown of  $\bar{R} \propto R$ .

An environment with intermediate expansion rates is provided by low-dimensionality forerunner structures, like filaments and sheets that modulate the matter distribution in the "field" into a quasi-linear cellular network. Inside, and especially at the intersections of such structures, the increased contrast allows aggregations to proceed and build up condensations. Then overall masses and time scales are set by the dynamics of such large-scale structures and of their intersections (see White & Ostriker 1990). We shall discuss these interesting conditions elsewhere.

## 6. CONCLUSIONS

A fully scale-invariant cluster evolution assumes the intra-cluster plasma (ICP) to scale with  $z$  just like the dynamical quantities (themselves scale-free). In the X-ray band the resulting cluster evolution is positive, or nearly neutral when  $\nu < -2$  holds (see Fig. 3), and this conflicts with existing observations, as discussed in § 1. So, some breaking of full-scale invariance is needed.

Our main point is that the gravitational clustering is likely to be scale-free, but the ICP physics is not. This is because nongravitational energy inputs from stellar formation and evolution can prevent for a while the baryons from clustering with dark matter. Thus the ICP constitutes a cluster component *younger* on average than the stars, and this strengthens negative evolution in the X-ray band.

Specifically, we discussed the canonical scenario of direct hierarchical collapses from small perturbations in a critical universe, with uniform primeval baryons but different light and mass distributions. Then, the scale invariance of the *gravitational* clustering is broken by *nuclear* energetics at masses  $M \lesssim 10^{13} M_\odot$ . Thereafter, the effects are *gradually* erased by the increasing dilution with diffuse baryons in progressively larger and deeper potential wells. Such baryons originate from a higher mass fraction available in diffuse form, with final density enhanced by the increasing compression factor  $n_2/n_1$  (see § 3).

Quantitatively,  $n_2/n_1(z)$  is sensitive to the redshift  $z_1$  at which the virial temperature  $T_2$  starts to depart from the temperature  $T_1$  of the infalling baryons. The state of the intergalactic medium is still loosely constrained (see Barcons, Fabian, & Rees 1991), so  $T_1$  may match  $T_2$  down to fairly modest redshifts. A negative evolution at  $z \approx 0.2-0.3$  as strong as indicated by the pre-ROSAT evidence requires ICP evolution, the faster the larger is  $\nu$ . So  $z_1 \approx 1.5-2$  is to hold, implying for the baryons protracted exposure to energy inputs of stellar origin and/or slowed down expansion. During the submission of the present work, a paper by Kaiser (1991) appeared, where a similar approach has been developed on the basis of the adiabatic approximation for  $n_2/n_1$ . For small  $T_1/T_2$  this approaches very closely the shock adiabat; the latter saturates to  $n_2/n_1 \rightarrow 4$  for large temperature ratios, while the Poisson adiabat keeps on rising, thus maximizing the effect. Conversion of gravitational energy by means of shocks, on the other hand, is supported by many different simulations of cluster collapses, from Perrenod (1980) to Evrard (1990), to Cen & Ostriker (1992). In

sum, in our view the clusters collect external baryons, and the amount of their negative evolution in the X-ray gauges the thermal state of the infalling IGM.

The second point we make is that the intrinsic dispersion in formation times tends to produce steeper LFs, rising their faint end (see § 4).

At a closer resolution, the above picture includes the following features:

1. The shape of the LFs agrees with the data for values of the spectral index  $-1.2 > \nu \gtrsim -1.7$  (see Figs. 2 and 3). Higher values produce LFs which are too steep, and lower values LFs which are too flat. The latter limit could be relaxed adopting a larger bias parameter  $b > 1.2$ . But physically motivated, "mixed" spectral models (see Taylor & Rowan-Robinson 1992, Davis, Summers, & Schlegel 1992) comply with the linear data on scales close to clusters with  $\nu < -1.2$  and  $b \lesssim 1.2$ ; "tilted" spectral models (Lucchin, Matarrese, & Mollerach 1992) with  $\nu \approx -1.4$  and  $b \approx 1.4$  also provide fitting LFs. Note that larger values of  $b$  would yield an optical anti-evolution conflicting with the evidence referred to in § 1.

2. The dynamical contribution to the antievolution of the bolometric X-ray luminosity  $L_c(z)$  is  $(1+z)^{(5+7\nu)/2(\nu+3)}$ . The ICP relative decrease contributes a factor  $(1+z)^{-2\xi}M^{0.4}$  (see § 2). The product will be observed at the bright end as a fast dearth of luminous clusters measured by  $N(z) \propto L_c^{\gamma_e-1}(z)/M_c(z)$ , with the time scale shortened by a factor  $1/(\gamma_e - 1)$  depending on the steep effective slope  $\gamma_e$  in the LF tail.

3. To agree with the data resolved out to  $z \sim 0.4$ , faster ICP evolution ( $\xi \approx 1$ ) is needed for  $\nu = -1.2$ , while for  $\nu \approx -1.7$  values  $\xi \approx 0.5$  are sufficient. Such combinations comply with the observational upper limits to the residual X-ray background in the 1/4–1 keV band (see the discussion by Burg, Cavaliere & Menci 1993), which probe the full path length out to  $z \sim 1$ . The dependence of  $g^2(M, z)$  on  $M$  is also important (see Burg et al. 1993) to yield the observed steep  $L-T$  correlation, approximately  $L \propto T^3$ .

4. The  $z$ -distributions expected from the ROSAT survey (see Böhringer et al. 1991) at fluxes  $F \gtrsim 10^{-13}$  ergs  $\text{cm}^{-2} \text{s}^{-1}$ , are shown in Figures 4 and 5.

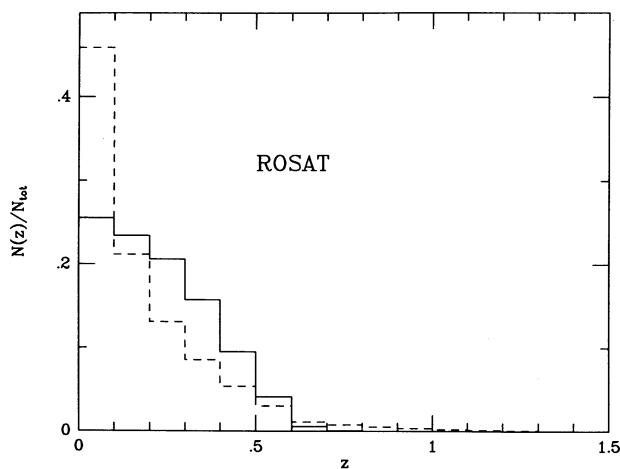


FIG. 4.—The  $z$ -distributions of clusters and groups as X-ray sources, corresponding to the models in Fig. 2 (dashed line) and in Fig. 3 (solid line). At small  $z$  the distributions are sensitive to the features of the LFs and to the flux range; the present plots have been computed for fluxes  $F \geq 5 \cdot 10^{-13}$  ergs  $\text{cm}^{-2}$  in the energy band of ROSAT.

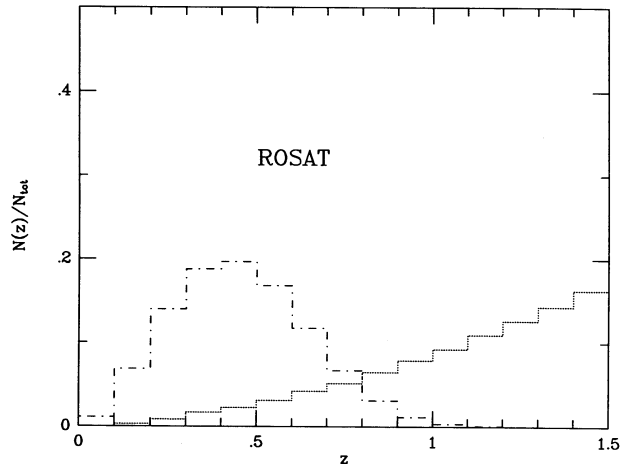


FIG. 5.—The  $z$ -distributions derived for groups and clusters at the same fluxes and with the same local LF as used for the solid line in Fig. 4, but with fully scale-invariant evolution (dotted line) or with no evolution (dot-dashed line).

5. Cooling flows at high  $z$  are limited by the relative dearth of ICP; the equivalent widths of high-excitation lines increase at  $z > 0$ .

We point out the consistent evidence of changes in the morphology and in the evolutionary rate of radio-loud quasars and radio galaxies in clusters at  $z \sim 0.3$ – $0.5$  (see Ellingson, Yee, & Green 1991; Hill & Lilly 1991). This has been interpreted as another effect of a rapid increase in pressure and density of the confining and stripping ICP.

At the opposite extreme, in an underdense universe dynamical collapses and ICP history tend to be slowed down into a nearly uniform distribution out to  $z \sim \Omega_0^{-1} - 1$ . At  $z \lesssim 0.5$ , this condition yields X-ray  $z$ -distributions with a decline not too far from our evolutionary picture for  $\Omega_0 = 1$ ; for a comparison, see Figures 4 and 5. But for  $\Omega_0 \ll 1$  the Sunyaev-Zel'dovich effect by the same X-ray-emitting ICP, when integrated along the line of sight and over a large beam, would produce an appreciable spectral distortion of the cosmic microwave background (Cavaliere, Menci, & Setti 1991; Markevitch et al. 1991). In fact, at wavelengths clear from radio-source or dust contamination, this is close to detectability with instruments like COBE/FIRAS. Considerably smaller distortions arise when dynamics and ICP follow the fully scale-invariant evolution, which instead gives excess counts at substantial  $z$  as shown in Figure 5. This striking difference in the high- $z$  contributions arises because different combinations of  $n$  and  $T$  are so probed:  $n^2 R^3 T^{1/2}$  by the X-ray counts, or  $\int dR nT$  by the SZ distortions.

In turn, the optical observations probe essentially the central dynamics. So, these three sets of data concerning different aspects of the same structures offer good opportunities for telling the history of the dynamical mass from that of the diffuse baryons.

We thank J. E. Pesce and R. Scaramella, and especially R. Burg and P. Tozzi, for useful discussions and comments, and the referee for help in the presentation. We acknowledge grants from ASI and MURST.

## APPENDIX

## DERIVATION OF THE LUMINOSITY FUNCTION

The luminosity  $L$  follows the scaling given by equation (4.3), from which we can express  $M$  in terms of  $\delta$  and  $L$  chosen as our independent variables. With this, the mass fraction in overdensities of given  $L$  and  $\delta$  reads

$$\Pi(L, \delta, z) M dL d\delta = \rho_a(z) \frac{d}{dL} \{p[\delta | \sigma(M)]\} d\delta dL, \quad (\text{A1})$$

where  $p[\delta | \sigma(M)]$  is the statistical distribution of the linear  $\delta$  filtered on the scale  $M$ .

First we assume for  $p[\delta | \sigma]$  the Gaussian shape

$$p(\delta | M) = \frac{1}{\sqrt{2\pi} \sigma} e^{-\delta^2/2\sigma^2} \quad (\text{A2})$$

with the variance  $\sigma = (M/M_c)^{-a}$ . Expressing  $M$  in terms of  $L$  and  $\delta$ , and collecting all  $\delta$ -dependences at the righthand side of equation (A1), we find for the number density  $N(L) \equiv \int_{\delta_c}^{\infty} d\delta \Pi(L, \delta)$  of condensations with a given  $L$  and  $\delta > \delta_c$  the expression:

$$N(L, z) = \frac{b\delta_c}{\sqrt{2\pi}} \frac{\rho_a}{M_c L_c} \ell^{-1/c} \frac{\partial}{\partial \ell} \ell^{ad/c(c-ad)} \int_{\ell^{a/(c-ad)}}^{\infty} d\zeta \zeta^{d(1-a)/(c-ad)} e^{\zeta^{2(1-ad/c)(b^2\delta_c^2/2)}}; \quad (\text{A3})$$

here  $\ell = L/L_c$  with  $L_c = g^2[M_c(z), z]M_c^c \rho_c^{7/6}$ , and  $\zeta = (\delta/\delta_c)\ell^{a/(c-ad)}$ .

Performing the derivative with respect to  $\ell$  yields

$$N(L, z) = A \frac{\rho_a(z)}{M_c(z)L_c(z)} \left[ \ell^{-1-(1-a)/c} e^{-b^2\delta_c^2\ell^{2a/c}/2} + C\ell^{-1-[1/(c-ad)]} \Gamma\left(q, \frac{b^2\delta_c^2}{2} \ell^{2a/c}\right) \right] \quad (\text{A4})$$

where the parameters read:

$$\begin{aligned} A &= 2b\delta_c a/\sqrt{2\pi}(c-ad), \\ C &= (b^2\delta_c^2/2)^q d/2(c-ad), \\ q &= [1 + d(1-a)/c]/2(1-ad/c). \end{aligned} \quad (\text{A5})$$

Note that in the limit of no  $\delta$ -dependence for  $L$  (i.e., when  $d = 0$ ) the second term vanishes and one recovers the canonical expression in equation (2.3).

A similar derivation is carried out starting from the height distribution of isolated peaks given by Bardeen et al. (1986), namely,

$$p(\delta | M) = \frac{1}{\sqrt{2\pi} \sigma} e^{-\delta^2/2\sigma^2} G\left(\frac{\delta}{\sigma}\right). \quad (\text{A6})$$

The function  $G(\delta/\sigma)$  is given by Bardeen et al. (1986). For  $\nu = -1.2$ , for example, this implies that the exponent of  $\ell$  is flattened to  $\approx -1.6$ .

## REFERENCES

- Abell, G. O. 1958, *ApJS*, 3, 211  
 Barcons, X., Fabian, A. C., & Rees, M. J. 1991, *Nature*, 350, 685  
 Bardeen, J. M., Bond, J. R., Kaiser, N., & Szalay, A. S. 1986, *ApJ*, 403, 15  
 Blumenthal, G., Faber, S. M., Primack, J. R., & Rees, M. J. 1984, *Nature*, 311, 517  
 Böhringer, H., et al. 1991, in *Proc. NATO ASI "Clusters and Superclusters of Galaxies"*, ed. A. C. Fabian (Dordrecht: Kluwer), 71  
 Burg, R., Cavaliere, A., & Menci, N. 1993, *ApJ*, 404, L55  
 Cavaliere, A., Gursky, H., & Tucker, W. H. 1971, *Nature*, 231, 437  
 Cavaliere, A., & Colafrancesco, S. 1988, *ApJ*, 331, 660  
 ———. 1990, in *Clusters of Galaxies* (Cambridge: Cambridge Univ. Press), 43  
 Cavaliere, A., Burg, R., & Giacconi, R. 1991, *ApJ*, 366, L61  
 Cavaliere, A., Colafrancesco, S., & Scaramella, R. 1991, *ApJ*, 380, 15  
 Cavaliere, A., Colafrancesco, S., & Menci, N. 1991, *ApJ*, 376, L37 (CM)  
 ———. 1992, *ApJ*, 392, 41 (CM)  
 Cavaliere, A., & Fusco-Femiano, R. 1976, *A&A*, 49, 137  
 Cavaliere, A., Menci, N., & Setti, G. 1991, *A&A*, 245, L21  
 Cen, R., & Ostriker, J. 1992, *ApJ*, 393, 22  
 Ciotti, L., D'Ercole, A., Pellegrini, S., & Renzini, A. 1991, *ApJ*, 376, 380  
 Cole, S., & Kaiser, N. 1989, *MNRAS*, 237, 1127  
 David, L. P., Arnaud, K. A., Forman, W., & Jones, C. 1990, *ApJ*, 356, 32  
 Davis, M., Summers, F. J., & Schlegel, D. 1992, *Nature*, 359, 393  
 Edge, A. C., & Stewart, G. C. 1991a, *MNRAS*, 252, 414  
 Edge, A. C., & Stewart, G. C. 1991b, *MNRAS*, 252, 428  
 Edge, A. C., Stewart, G. C., Fabian, A. C., & Arnaud, K. A. 1990, *MNRAS*, 245, 559  
 Ellingson, E., Yee, H. K. C., & Green, R. F. 1991, *ApJ*, 371, 49  
 Ellis, R. G. 1991, in *Traces of the Primordial Structure of the Universe*, ed. H. Böhringer & R. H. Treumann (Munich: MPE Report), 101  
 Evrard, A. 1990, *ApJ*, 363, 349  
 Fabbiano, G. 1989, *ARA&A*, 27, 87  
 Fabian, A. C. 1991, in *Proc. NATO ASI "Clusters and Superclusters of Galaxies"*, ed. A. C. Fabian (Dordrecht: Kluwer), 151  
 Frenk, C. S., White, S. D. M., Efstathiou, G., & Davis, M. 1990, *ApJ*, 351, 10  
 Gioia, I. M., Henry, J. P., Maccacaro, T., Morris, S. L., Stocke, J. T., & Wolter, A. 1990, *ApJ*, 356, L35  
 Gunn, J. 1990, in *Clusters of Galaxies* (Cambridge: Cambridge Univ. Press), 341  
 Gursky, H., Solinger, A., Kellogg, E., Murray, S., Tananbaum, H., Giacconi, R., & Cavaliere, A. 1972, *ApJ*, 173, L99  
 Henry, J. P., Gioia, I. M., Maccacaro, T., Morris, S. L., Stocke, J. T., & Wolter, A. 1992, *ApJ*, 386, 408  
 Hill, G. J., & Lilly, S. J. 1991, *ApJ*, 367, 1  
 Hoffman, Y., Shaham, J., & Shaviv, G. 1982, *ApJ*, 262, 413  
 Kaiser, N. 1984, *ApJ*, 284, L49  
 ———. 1986, *MNRAS*, 222, 323

- Kaiser, N. 1991, ApJ, 383, 104  
Kowalski, M. P., Ulmer, M. P., Cruddace, R. G., & Wood, K. S. 1984, ApJS, 56, 403  
Landau, L. D., & Lifshitz, E. M. 1959, Fluid Mechanics (London: Pergamon)  
Lucchin, F., Matarrese, S., & Mollerach, S. 1992, preprint  
Markevitch, M., Blumenthal, G. R., Forman, W., Jones, C., & Sunyaev, R. A. 1991, ApJ, 378, L33  
Olivier, S., Blumenthal, G. R., Deckel, A., Primack, J. R., Stanhill, D. 1990, ApJ, 356, 1  
Peebles, P. J. 1980, The Large Scale Structure of the Universe (Princeton: Princeton Univ. Press)  
Perrenod, S. C. 1978, ApJ, 226, 566  
———. 1980, ApJ, 236, 373  
Piccinotti, G., Mushotzky, R. F., Boldt, E. A., Holt, S. S., Marshall, F. E., Serlemitsos, P. J., & Shafer, R. A. 1982, ApJ, 253, 485  
Press, W. H., & Schechter, P. 1974, ApJ, 187, 425  
Sarazin, C. L. 1988, X-ray Emission from Clusters of Galaxies (Cambridge: Cambridge Univ. Press)  
Scaramella, R., Vettolani, G., Zamorani, G., & Chincarini, G. 1990, AJ, 101, 342  
Solinger, A. B., & Tucker, W. H. 1972, ApJ, 175, L107  
Taylor, A. N., & Rowan-Robinson, M. 1992, Nature, 359, 396  
Trinchieri, G., & Fabbiano, G. 1985, ApJ, 296, 447  
Trümper, J., et al. 1991, A&A, 246, L1  
White, S. D. M., & Ostriker, J. P. 1990, ApJ, 349, 22